Naval Research Laboratory
Washington, DC 20375-5320

NRL/8230/MR—2022/2

Applications of Adaptive Non-Singular Terminal Sliding Mode Control to Rendezvous with Malfunctioning Clients

BRYAN PATRIC HOSKINS

Dynamics and Control Systems Branch
Spacecraft Engineering Division

September 25, 2022

DISTRIBUTION STATEMENT A: Approved for public release; distribution is unlimited.

REPORT DOCUMENTATION PAGE

Form Approved
OMB No. 0704-0188

Public reporting burden for this collection of information is estimated to average 1 hour per response, including the time for reviewing instructions, searching existing data sources, gathering and maintaining the data needed, and completing and reviewing this collection of information. Send comments regarding this burden estimate or any other aspect of this collection of information, including suggestions for reducing this burden to Department of Defense, Washington Headquarters Services, Directorate for Information Operations and Reports (0704-0188), 1215 Jefferson Davis Highway, Suite 1204, Arlington, VA 22202-4302. Respondents should be aware that notwithstanding any other provision of law, no person shall be subject to any penalty for failing to comply with a collection of information if it does not display a currently valid OMB control number. **PLEASE DO NOT RETURN YOUR FORM TO THE ABOVE ADDRESS.**

1. REPORT DATE *(DD-MM-YYYY)*	**2. REPORT TYPE**	**3. DATES COVERED** *(From - To)*
25-09-2022	NRL Memorandum Report	08/03/2021 – 08/03/2022

4. TITLE AND SUBTITLE

Applications of Adaptive Non-Singular Terminal Sliding Mode Control to Rendezvous with Malfunctioning Clients

5a. CONTRACT NUMBER

5b. GRANT NUMBER

5c. PROGRAM ELEMENT NUMBER
NISE

6. AUTHOR(S)

Bryan Patric Hoskins

5d. PROJECT NUMBER

5e. TASK NUMBER

5f. WORK UNIT NUMBER
N20N

7. PERFORMING ORGANIZATION NAME(S) AND ADDRESS(ES)

Naval Research Laboratory
4555 Overlook Avenue, SW
Washington, DC 20375-5320

8. PERFORMING ORGANIZATION REPORT NUMBER

NRL/8230/MR--2022/2

9. SPONSORING / MONITORING AGENCY NAME(S) AND ADDRESS(ES)

Naval Research Laboratory
4555 Overlook Avenue, SW
Washington, DC 20375-5320

10. SPONSOR / MONITOR'S ACRONYM(S)
NRL-NISE

11. SPONSOR / MONITOR'S REPORT NUMBER(S)

12. DISTRIBUTION / AVAILABILITY STATEMENT

DISTRIBUTION STATEMENT A: Approved for public release; distribution is unlimited.

13. SUPPLEMENTARY NOTES

Karles Fellowship

14. ABSTRACT

This paper presents the research performed within the first year of a Karle's Fellowship, which investigates how to autonomously control an inspection vehicle towards a malfunctioning client to accomplish inspection related tasks. The objective of this research is to develop a finite-time relative position control framework to enable an inspection satellite to safely approach a malfunctioning client vehicle, whose ability to communicate has been hindered, rendering it unable to communicate at all during a proximity maneuver. Malfunctioning clients present unique challenges, namely that the state of the client is considered unknown a priori and the inspector may not benefit from accurate and continuous information provided by the client vehicle; the client vehicle may also be subject to maneuvering and disturbances, unknown to the inspector a priori.

15. SUBJECT TERMS

Adaptive control
Autonomous R&D
Terminal sliding mode control
Nonlinear spacecraft dynamics
Spacecraft position control

16. SECURITY CLASSIFICATION OF:			**17. LIMITATION OF ABSTRACT**	**18. NUMBER OF PAGES**	**19a. NAME OF RESPONSIBLE PERSON**
a. REPORT	**b. ABSTRACT**	**c. THIS PAGE**			Bryan P. Hoskins
U	U	U	U	18	**19b. TELEPHONE NUMBER** *(include area code)* (202) 404-4374

Standard Form 298 (Rev. 8-98)
Prescribed by ANSI Std. Z39.18

This page intentionally left blank.

U.S. NAVAL RESEARCH LABORATORY

Applications of Adaptive Non-Singular Terminal Sliding Mode Control to Rendezvous with Malfunctioning Clients

Bryan Hoskins, Code 8233

This paper presents the research performed within the first year of a Karle's Fellowship, which investigates how to autonomously control an inspection vehicle towards a malfunctioning client to accomplish inspection related tasks. The objective of this research is to develop a finite-time relative position control framework to enable an inspection satellite to safely approach a malfunctioning client vehicle, whose ability to communicate has been hindered, rendering it unable to communicate at all during a proximity maneuver. Malfunctioning clients present unique challenges, namely that the state of the client is considered unknown *a priori* and the inspector may not benefit from accurate and continuous information provided by the client vehicle; the client vehicle may also be subject to maneuvering and disturbances, unknown to the inspector *a priori*.

During the first term of this fellowship, simulation software was developed using MATLAB and Simulink to demonstrate an inspection vehicle performing a rendezvous maneuver with a malfunctioning client vehicle. A line-of-sight based relative motion model is firstly introduced, which uses the navigation information directly, then a robust control framework is developed in the form of an adaptive non-singular terminal sliding mode controller to ensure the closed loop system is stable and to guarantee finite-time convergence to the desired states. The simulation results are then presented and discussed before finally discussing future work and objectives.

Contents

Distribution Statement A. Approved for public release, distribution is unlimited.

BACKGROUND AND MOTIVATION

Interest in space technologies that enable an inspection vehicle to approach and operate near malfunctioning clients has seen a sharp increase in recent years; orbiting debris and the number of deactivated satellites has increased substantially in the last decade and as such, the threat posed to indispensable space assets has also sharply increased.

The Orbital Express program sponsored by the Defense Advanced Research Projects Agency (DARPA) demonstrated on-orbit servicing as well as several other technological milestones, using a servicing vehicle known as ASTRO (Autonomous Space Transfer and Robotic Orbiter) and a client vehicle known as NextSat (Next generation Satellite). However, this demonstration assumed the client vehicle had the ability to assist in the on-orbit servicing maneuver via transponders and optical reflective geometry. Satellite formation control remains challenging regardless of the nature of the client vehicle, and a broader understanding of how to operate around malfunctioning clients is necessary[1,2,3].

Operating autonomously near these malfunctioning, potentially hazardous bodies introduces unique challenges that must be solved to ensure a successful mission; for example, these malfunctioning client vehicles have the potential to be damaged, and therefore could be subject to small translational maneuvering or tumbling from a damaged reaction control thruster. This specific scenario is challenging and the enabling technologies are comparatively under-developed, when compared to the autonomous capabilities of inspection vehicles executing on-orbit inspection with functional clients, capable of assisting the inspection vehicle in some manner.

With the goal of reducing operator intervention, literature has provided several techniques and approaches to the inherently challenging problem of autonomously maneuvering an inspection vehicle around its designated client vehicle. However, the area of research related to malfunctioning clients faces many technical challenges which include dynamic modeling, guidance, navigation and control, sensing and actuator limitations as well as simulation and validation[3].

TECHNICAL OBJECTIVE

The objective of this study is to develop an autonomous, high fidelity control strategy which can maneuver an inspection satellite from moderate initial separations into a close proximity passive parking orbit, about a possibly malfunctioning client; for inspection, mapping, imaging and data collection objectives. The inspection vehicle shall be capable of reacting to unknown and uncontrolled client maneuvering during rendezvous and proximity operations, and remain in proximity until all mission objectives are satisfied, at which point the inspector shall depart. Understanding how to maneuver an

[1] R. B. Friend, "Orbital Express program summary and mission overview," in Sensors and Systems for Space Applications II, Apr. 2008, vol. 6958, pp. 11–21

[2] K. Zhang, G. Duan, and M. Ma, Adaptive sliding-mode control for spacecraft relative position tracking with maneuvering target, International Journal of Robust and Nonlinear Control, vol. 28, no. 18, pp. 5786–5810, 2018

[3] Z. Jing, R. Pan, Y. Li, and P. Dong, Non-Cooperative Target Tracking, Fusion and Control. 2018

Manuscript approved September 13, 2022.

Distribution Statement A. Approved for public release, distribution is unlimited.

inspection vehicle within proximity of a malfunctioning clients is paramount to the future of space flight; this research recognizes a significant gap in relevant literature. Therefore, the results of this research will not only lay the foundation for future exploration in this field and lead to the development of future modeling and simulation software, but potentially lead to future flight demonstrations and operational use.

TERMINOLOGY

Inspector: A controlled space vehicle that is authorized to conduct on-orbit inspection with a designated malfunctioning client.

Client: An un-controlled orbiting body or space vehicle that is designated as malfunctioning, hindered from assisting the inspector at all during a maneuver.

Malfunctioning: State of the client, which is rendered inoperable by some means and is unable to assist in a maneuver.

Earth Centered Inertial (ECI) Coordinate Frame: Inertial coordinate system attached to the Earth's center of mass and defined as $O_{x_I y_I z_I}$, with respect to EME2000, where $x_I - y_I$ define the equatorial plane with x_I pointing through the vernal equinox and z_I pointing through the North Pole[4,5].

Line-Of-Sight (LOS) Coordinate Frame: See "Defining Line-Of-Sight Coordinate System" section.

NOTATION

This research uses standard vector notion, position vector $r_{P/O}$ denotes the position of point *P* relative to *O*, with ECI coordinates being implied and assumed henceforth, unless stated otherwise. To properly define velocity and acceleration vectors, reference frames will be introduced; for example, velocity vector ${}^{L}\dot{r}_{P/O}$ is read as the velocity of point *P* relative to point *O* with respect to the LOS frame. Rotation matrices are used to convert between different coordinate systems; a rotation matrix that describes the LOS frame relative to the ECI frame is written as R_L^I.

[4] B. Schutz, B. Tapley, and G. H. Born, *Statistical Orbit Determination*. Elsevier, 2004.

[5] N. R. Boone and R. A. Bettinger, "Artificial Debris Collision Risk Following a Catastrophic Spacecraft Mishap in Lunar Orbit," p. 12, 2021.

Distribution Statement A. Approved for public release, distribution is unlimited.

DYNAMIC MODELING AND CONTROL METHODOLOGY

Defining Line-Of-Sight Coordinate System

The nature of the malfunctioning client implies that it does not assist the inspection vehicle during rendezvous and consequently, the client's orbital state could be partially or completely unknown; because of this, it is more convenient to formulate the dynamic model in a frame attached to the inspection vehicle[2]. This approach almost entirely removes the dependency on the client's orbital state, unlike a dynamic expression built in the client's reference frame; the remaining term containing the client's orbital state information can then be treated as an unknown bounded uncertainty within the control law design.

Defining a line-of-sight (LOS) coordinate frame attached to the inspector, not the unknown client, as depicted in **Figure 1**, would not only have more physical significance, but would reduce the computational complexity of having to convert the navigation information into a Cartesian frame[6]. This unconventional approach has been demonstrated in literature for several different applications, where each assumed that the client could potentially behave in a manner unknown to the inspector[2,6,7,8].

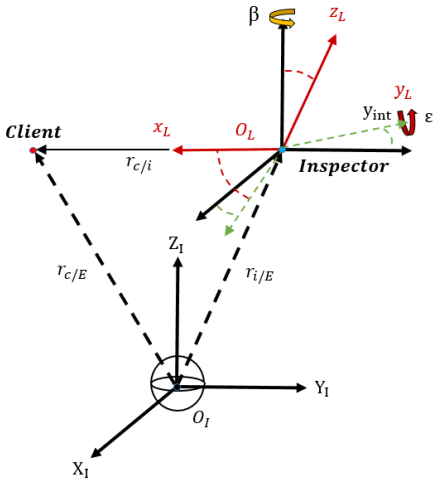

Figure 1: Line-of-sight reference frame

[6] F. Han, Z. Wang, Y. Han, and C. Liu, "Angles-Only Relative Navigation in Spherical Coordinates Using Unscented Kalman Filter," in *2020 39th Chinese Control Conference (CCC)*, Jul. 2020, pp. 3444–3451.

[7] P. Zhang and X. Zhang, "A novel adaptive three-dimensional finite-time guidance law with terminal angle constraints for interception of maneuvering targets," *International Journal of Control*, vol. 95, no. 6, pp. 1590–1599, Jun. 2022.

[8] B. Jiang, Q. Hu, and M. I. Friswell, "Fixed-time rendezvous control of spacecraft with a tumbling target under loss of actuator effectiveness," *IEEE Transactions on Aerospace and Electronic Systems*, vol. 52, no. 4, pp. 1576–1586, Aug. 2016.

Distribution Statement A. Approved for public release, distribution is unlimited.

The relevant navigation information includes the range (ρ) and two LOS angular measurements (β, ϵ) which are acquired through laser and optical sensors respectively. The navigation information can be used directly in the dynamic equations of relative motion when built in a spherical coordinate system, this is depicted in **Figure 1**.

The Earth centered inertial (ECI) coordinate system ($O_{x_I y_I z_I}$) can be related to the LOS rotating frame ($O_{x_L y_L z_L}$) through two rotations β ∈ (-π, π) and ε ∈ (-π/2, π/2); this encompasses an initial rotation about z_I by β, followed by a second rotation about y_{int} of the intermediate frame by -ε. The rotation matrices which relate the LOS coordinate frame to the ECI coordinate frame are shown in **(1).**

$$R_L^I = \begin{bmatrix} \cos(-\varepsilon) & 0 & -\sin(-\varepsilon) \\ 0 & 1 & 0 \\ \sin(-\varepsilon) & 0 & \cos(-\varepsilon) \end{bmatrix} \begin{bmatrix} \cos(\beta) & \sin(\beta) & 0 \\ -\sin(\beta) & \cos(\beta) & 0 \\ 0 & 0 & 1 \end{bmatrix} = \begin{bmatrix} \cos(\varepsilon)\cos(\beta) & \cos(\varepsilon)\sin(\beta) & \sin(\varepsilon) \\ -\sin(\beta) & \cos(\beta) & 0 \\ -\sin(\varepsilon)\cos(\beta) & -\sin(\varepsilon)\sin(\beta) & \cos(\varepsilon) \end{bmatrix} \quad (\mathbf{1})$$

Dynamic Model

In literature, a common approach to modeling satellite relative motion is to formulate the relative motion dynamics in the Hill frame, attached to the client satellite; these include the well-known Hill-Clohessy-Wiltshire and Tschauner-Hemple equations. However, as discussed in the previous section using a relative motion expression built in a rotating frame, attached to the inspection vehicle can be advantageous. Creating this expression is rather straightforward, starting from the ECI based relative position vector $r_{c/E} = r_{i/E} + r_{c/i}$ and using the transport theorem, **(2)** can firstly be derived.

$$\boldsymbol{{}^I\ddot{r}_{c/E} = {}^I\ddot{r}_{i/E} + {}^L\ddot{r}_{c/i} + {}^I\dot{\omega}^L \times r_{c/i} + 2{}^I\omega^L \times {}^L\dot{r}_{c/i} + {}^I\omega^L \times ({}^I\omega^L \times r_{c/i})} \quad (\mathbf{2})$$

Both the client's relative position and the angular velocity of the LOS frame about the ECI frame can be expressed in the LOS frame, as shown in **(3)**; the relative motion of the client relative to inspector in the ECI frame is also straightforward to formulate using Newton's Second Law as shown in **(4)**.

$$r_{c/i}^L = \begin{bmatrix} \rho \\ 0 \\ 0 \end{bmatrix} \quad {}^I\omega^L = \begin{bmatrix} \dot{\beta}\sin\varepsilon \\ -\dot{\varepsilon} \\ \dot{\beta}\cos\varepsilon \end{bmatrix} \quad (\mathbf{3})$$

$${}^I\ddot{r}_{c/i} = {}^I\ddot{r}_{c/E} - {}^I\ddot{r}_{i/E} = -\left(\frac{\mu}{\|r_{c/E}\|^3} r_{c/E} - \frac{\mu}{\|r_{s/E}\|^3} r_{i/E}\right) + \frac{1}{m_i}\left(\frac{m_i}{m_c} F_c - (F_i + F_d)\right) \quad (\mathbf{4})$$

Finally, the dynamic equations of relative motion written in the inspector's LOS frame can be acquired by substituting **(3)** and **(4)** into **(2)**; where $\boldsymbol{F_c}$, $\boldsymbol{F_i}$ and $\boldsymbol{F_d}$ are the client's thrusting, inspector's thrusting and external disturbances respectively. It is important to remember that **(4)** must be transformed into the appropriate coordinate frame using **(1)**, which is a transform from ECI coordinates to the new LOS-based

Distribution Statement A. Approved for public release, distribution is unlimited.

coordinate system[9]. The new equation shown in **(5)** can be used to describe the relative motion in spherical coordinates, with the inspector's thrust vector $\boldsymbol{u}$ and state vector $\boldsymbol{q} = [\boldsymbol{\rho} \quad \boldsymbol{\beta} \quad \boldsymbol{\varepsilon}]^{\boldsymbol{T}}$; where

$$\ddot{\boldsymbol{q}} = \boldsymbol{F} + \boldsymbol{B}\boldsymbol{u} + \boldsymbol{D} \tag{5}$$

and

$$\boldsymbol{F} = \begin{bmatrix} \rho\left(\dot{\varepsilon}^2 + \dot{\beta}^2 \cos^2 \varepsilon\right) \\ \dfrac{-2\dot{\rho}\dot{\beta} \cos \varepsilon + 2\rho\dot{\varepsilon}\dot{\beta} \sin \varepsilon}{\rho \cos \varepsilon} \\ \dfrac{-2\dot{\rho}\dot{\varepsilon} - \rho\dot{\beta}^2 \sin \varepsilon \cos \varepsilon}{\rho} \end{bmatrix},$$

$$\boldsymbol{B} = -\begin{bmatrix} \dfrac{1}{m_i} & 0 & 0 \\ 0 & \dfrac{1}{m_i \rho \cos \varepsilon} & 0 \\ 0 & 0 & \dfrac{1}{m_i \rho} \end{bmatrix},$$

$$\boldsymbol{D} = -\frac{m_i \mu}{\left\| r_{i/E} \right\|^3}\left(r^L_{c/i} - 3\frac{r^L_{c/i} \cdot r^L_{i/E}}{\left\| r_{i/E} \right\|^2} r^L_{i/E} \right) + \frac{m_i}{m_c}\boldsymbol{F_c^L} - \boldsymbol{F_d^L} = m_i \Delta \boldsymbol{g}^L + \frac{m_i}{m_c}\boldsymbol{F_c^L} - \boldsymbol{F_d^L}.$$

$\boldsymbol{F}$ and $\boldsymbol{B}$ are known quantities whereas disturbance term $\boldsymbol{D}$ is a lumped uncertainty, which include the gravity differential term $\Delta \boldsymbol{g}^L$, client thrusting term $\boldsymbol{F_c^L}$ and external disturbance term $\boldsymbol{F_d^L}$; similar formulations can be found in literature[2,7]. The disturbance term satisfies $\|\boldsymbol{D}\| \leq c_1 + c_2\|\boldsymbol{q}\|$ where c_1 and c_2 are the unknown bounds of the gravity differential, client maneuvering and external disturbances; which can then be treated as an unknown bounded uncertainty within the control law design. These bounds are unknown but considered finite; therefore, c_1 and c_2 can be expressed in **(6)** with $\left\|\boldsymbol{F_d^L}\right\| \leq b_1$, $\left\|\boldsymbol{F_c^L}\right\| \leq b_2$ and $\|\Delta g^L_{max}\| \leq b_3\|\boldsymbol{q}\|$.

$$c_1 = b_1 + \frac{m_i}{m_c} b_2,\ c_2 = m_i b_3 \tag{6}$$

For practical applications b_1 and b_3 are small and can be estimated beforehand, whereas the upper bound on the clients unknown thrusting, b_2, could be large and unknown *a-priori*; because of this, it is advantageous to create a control methodology without prior knowledge of disturbance bounds[2].

[9] For additional details see: J. Guo, Y. Li, and J. Zhou, "A new continuous adaptive finite time guidance law against highly maneuvering targets," Aerospace Science and Technology, vol. 85, pp. 40–47, Feb. 2019.

Distribution Statement A. Approved for public release, distribution is unlimited.

Control Methodology

Sliding mode control is a two phase, robust control method that is used to drive and constrain the motion of a system to a manifold called the sliding manifold, where the dynamics of the system are well behaved. This means driving the system to a manifold where the original dynamics are already stable; a visualization is shown in **Figure 2**[10]. During the reaching phase the control law is designed to drive the trajectories of the system to the sliding manifold; once on the manifold the sliding phase begins where the trajectories are confined and will slide along it until they reach the origin. The sliding mode control law is designed using this manifold, and must stabilize the origin, and therefore must be proven stable in the sense of Lyapunov; a suitable Lyapunov candidate function is typically the positive definite quadratic expression of the total energy. Using the LOS-based relative motion model derived in **(5)**, the stability of the system can be proven using the defined sliding manifold and control law; this is accomplished by differentiating the candidate function and proving negative definiteness.

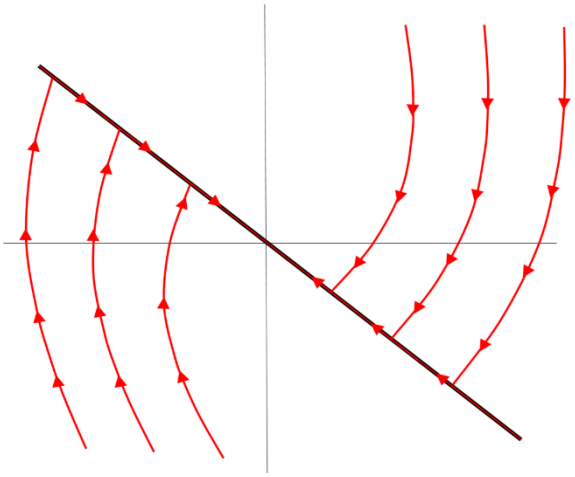

Figure 2: Phase portrait: sliding manifold s = 0 (black) and system trajectories (red)

The concept of sliding mode control is rooted in terminal attractors, meaning the trajectories of the system are driven to the sliding manifold, defined by $\boldsymbol{s} = 0$; the challenge lies in building desirable characteristics and properties into this manifold. One desirable property built into the sliding manifold is finite-time convergence, which ensure that the states of the system arrive at equilibrium in finite time once sliding mode is achieved. To ensure that the system converges to the desired states in finite-time the concept of terminal sliding mode control (TSMC) is introduced. Define the desired state vector as $\boldsymbol{q_d} = [\rho_d \quad \beta_d \quad \varepsilon_d]^{\boldsymbol{T}}$ and define the tracking error as $\boldsymbol{e} = \boldsymbol{q} - \boldsymbol{q_d}$, then the manifold used to drive the trajectories to the sliding mode in finite-time can be defined by

$$\boldsymbol{s} = \boldsymbol{e} + \alpha|\dot{\boldsymbol{e}}|^{\lambda} sign(\dot{\boldsymbol{e}}) = 0, \tag{7}$$

where $\alpha > 0$ and $1 < \lambda < 2$. This expression is one of many variations that reach equilibrium in finite-time, but it is important to understand that this form avoids singularities that arise, as sliding mode control requires the derivative of **(7)**[11]. The finite-time reachability property defined as

$$T = \frac{\alpha^{\frac{1}{\lambda}}|\boldsymbol{e_0}|^{1-\frac{1}{\lambda}}}{1-\frac{1}{\lambda}}, \tag{8}$$

[10] For additional details on sliding mode control see: Khalil, Hassan K. Nonlinear Systems. Third ed., Prentice Hall, 2002.

[11] X. Yu, Y. Feng, and Z. Man, "Terminal Sliding Mode Control – An Overview," IEEE Open Journal of the Industrial Electronics Society, vol. 2, pp. 36–52, 2021.

Distribution Statement A. Approved for public release, distribution is unlimited.

shows that once the sliding mode is achieved, i.e. $\boldsymbol{s} = 0$, the state error trajectories will converge to $\boldsymbol{e} = 0$ from any initial error state $\boldsymbol{e_0}$ in finite-time[12,13]. Recall that the client's malfunctioning nature inhibits knowledge of the bounded uncertainties; therefore, some type of dynamic adaptation is required to prevent gain overestimation and excessively large control signals. The adaptive non-singular terminal sliding mode controller (ANTSMC) can be introduced as

$$\boldsymbol{u} = \boldsymbol{B}^{-1}\left(\boldsymbol{F} + \alpha^{-1}\lambda^{-1}|\dot{\boldsymbol{e}}|^{2-\lambda} sign(\dot{\boldsymbol{e}}) + k\boldsymbol{s} + \eta(t)\tanh(\frac{\boldsymbol{s}}{\delta})\right), \tag{9}$$

where $k = diag(k_1, k_2, k_3)$ and $k_1, k_2, k_3 > 0$. The adaptive, dynamically tuned control gain, written as $\eta(t)$, counteracts parameter uncertainties and unknown, but bounded disturbances. The adaptation laws updated the adaptive gain and provide the necessary robustness to ensure high precision when in the presence of external disturbances whose bounds are finite, but unknown *a priori*. The adaptive laws prevents gain over estimation, ensuring the control gain is as small as possible while still preserving the stability of the system, the adaptive control gain and adaptation laws are defined as

$$\boldsymbol{s} \geq \boldsymbol{\delta} \tag{10}$$

$$\eta(t) = \hat{c}_1 + \hat{c}_2\|\boldsymbol{q}\|$$

$$\dot{\hat{c}}_1 = \bar{\kappa}_1\|s\|$$

$$\dot{\hat{c}}_2 = \bar{\kappa}_2\|s\|\|\boldsymbol{q}\|$$

and

$$\boldsymbol{s} < \boldsymbol{\delta} \tag{11}$$

$$\eta(t) = (\hat{c}_1 + \hat{c}_2\|\boldsymbol{q}\|)\|\zeta\| + \bar{\kappa}_3$$

$$\dot{\hat{c}}_1 = 0$$

$$\dot{\hat{c}}_2 = 0$$

$$\dot{\zeta} = \frac{1}{\tau}\left(\tanh\left(\frac{s}{\delta}\right) - \zeta\right).$$

It is important to mention that sliding mode control will only drive the trajectories of the system to a region around the sliding manifold; because of this, rapid switching above and below the sliding manifold occurs, resulting in a phenomena known as chattering; having the adaptive laws behave differently depending on the proximity to the sliding manifold helps eliminate this effect. Chattering causes reduced control accuracy and high heat loss in electronics and in turn wear on mechanical parts, degrading system

[12] Y. Hong, J. Huang, and Y. Xu, "On an output feedback finite-time stabilization problem," *IEEE Transactions on Automatic Control*, vol. 46, no. 2, pp. 305–309, Feb. 2001.
[13] S. Yu, X. Yu, B. Shirinzadeh, and Z. Man, "Continuous finite-time control for robotic manipulators with terminal sliding mode," *Automatica*, vol. 41, no. 11, pp. 1957–1964, Nov. 2005.

Distribution Statement A. Approved for public release, distribution is unlimited.

performance. To mitigate the control demand and further reduce chattering effects, the control law can be supplemented with a high slope saturation function or a hyperbolic tangent function.

This control approach went through several iterations before the current adaptive non-singular terminal sliding mode controller was developed; each variation proved to be a valuable comparison metric as the control strategy evolved. Sliding mode control was firstly investigated, which used a linear sliding surface; however, it was determined that the approach was not robust enough to handle the levels of uncertainty being considered. Therefore, adaptive laws were implemented to create an adaptive sliding mode control law which can handled large uncertainties, reduce controller demand and chattering effects as well as improving both performance and convergence. To further improve the convergence rate, terminal sliding mode control theory was investigated, which led to the development of an adaptive terminal sliding mode control law. Finally, recognizing that the developed control approach could encounter singularities, resulting in an infinity large control signal, the non-singular property was introduced into the sliding manifold to create the current adaptive non-singular terminal sliding mode control law.

Simulation Overview

Simulink proved to be an incredibly useful and versatile tool for developing control simulations, and translating the above approach into Simulink, in and of itself, albeit tedious, was not challenging; the simulation's Simulink flow diagram is shown in **Figure 3**. All control parameters, adaptive law parameters, orbital parameters and initial conditions are initialized through a single parameter file which Simulink calls and executes at the start of the simulation. Currently the capability to accommodate for

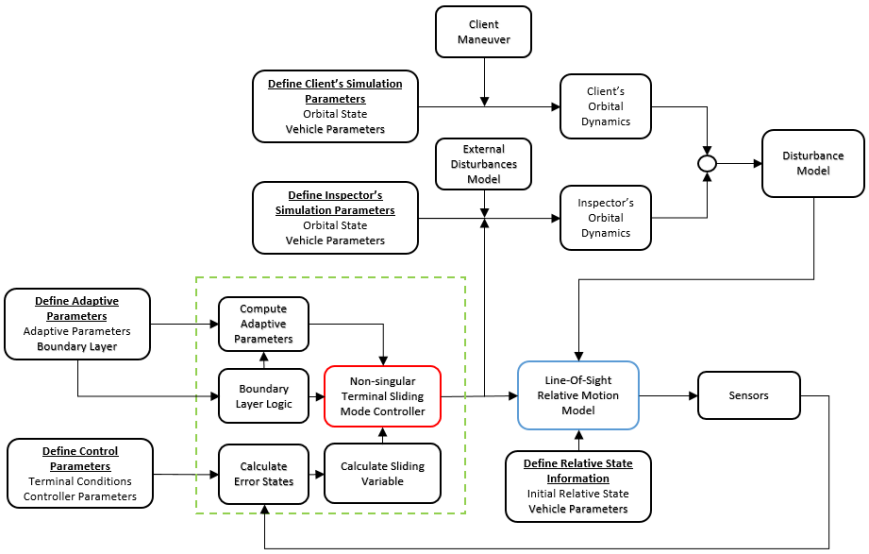

Figure 3: Simulink flow diagram

Distribution Statement A. Approved for public release, distribution is unlimited.

client maneuvering is still in the verification and validation (V&V) stage and has yet to be deployed into the current simulation.

The disturbance model for the LOS-based relative motion propagator is first calculated; this model, shown in **(5)**, contains the gravity differential term, external perturbations and client thrusting terms. Recall that the approach used in this research does not require knowledge of the client vehicle as the LOS-based coordinate system removes the dependency on the client's orbital state and that the LOS-based spherical states $\boldsymbol{q} = [\boldsymbol{\rho} \quad \boldsymbol{\beta} \quad \boldsymbol{\varepsilon}]^{\boldsymbol{T}}$ can be measured directly using the inspector's on-board sensor suite; in practical applications the malfunctioning nature of the client will inhibit communication with the inspector. However, for the purpose of the simulation both the client and inspector's orbital states are propagated and used to create an accurate disturbance model for the LOS-base relative motion propagator; the disturbance term **D** in **(5)** can then be treated as an uncertainty within the control law design.

Once calculated, the disturbance model is fed into the relative motion propagator where the LOS states are propagated forward in time. Using the disturbance model and the propagated LOS states the error state $\boldsymbol{e}$ is calculated which is used to update the sliding variable $\boldsymbol{s}$; the sliding variable defines where the system trajectories are in relation to the sliding manifold. These values are then used to calculate the controller's adaptive gain and control signal. The control gain must be dynamically tuned to improve the performance of the controller; a larger control gain means the inspector will be thrusting more than necessary to perform the rendezvous maneuver. The adaptive gain is calculated using the series of adaptive laws shown in **(5)**, which ensure that the control gain remains small while still ensuring stability. The adaptive gain then feeds directly into the non-singular terminal sliding mode controller to update the relative state.

RESULTS AND DISCUSSION

Although the simulation developed during this research is still evolving, part of the original objective has already been satisfied. Therefore, this section will present the results of three scenarios, applying the suggested ANTSMC approach to simulated rendezvous maneuvers to achieve the desired terminal states. The client and inspector's orbital elements for the first two scenarios are shown in **Table 1**; where a is the semi-major axis, e is the eccentricity, i is the inclination, ω is the argument of periapsis, Ω is the right ascension of the ascending node and θ is the true anomaly. The orbital elements can be derived using the user defined initial states, shown in **(11)**.

$$\boldsymbol{q_0} = \begin{bmatrix} 60\ m \\ -0.1228\ rad \\ 0.1166\ rad \end{bmatrix}, \quad \dot{\boldsymbol{q}}_{\boldsymbol{0}} = \begin{bmatrix} 4.907 \times 10^{-3}\ {}^{m}/_{s} \\ 1.295 \times 10^{-3}\ {}^{rad}/_{s} \\ 0.018 \times 10^{-3}\ {}^{rad}/_{s} \end{bmatrix} \tag{11}$$

For the first two scenarios the inspection vehicle is assumed to be small (~50 kg) with thrusting limitations of ± 10 N, for the purpose of the simulation the client is assumed larger (~200 kg). The external disturbances acting on the inspection vehicle are assumed small.

Distribution Statement A. Approved for public release, distribution is unlimited.

	a (km)	e	i (°)	Ω (°)	ω (°)	Θ (°)
Client	7200	0.15	15	45	10	30
Inspector	7200	0.15	14.9999	45.0006	10	29.9999

Table 1: Client and inspector's orbital elements (Scenario 1 and 2)

Scenario 1:

To demonstrate the effectiveness of the proposed ANTSMC law, a simple rendezvous maneuver is simulated, requiring the inspector to reach a holding position behind the client; the desired terminal states are shown in **(12)** requiring the inspector to maneuver 5 meters behind the client vehicle.

$$\boldsymbol{q_d} = \begin{bmatrix} 5\ m \\ 0\ rad \\ 0\ rad \end{bmatrix} \tag{12}$$

The sliding surface parameters which are used to tune the controller's convergence rate to the terminal states are set as follows, $\alpha = diag([25 \quad 15 \quad 15])$ and $\lambda = 1.1$; the control parameters $\boldsymbol{k}$ and $\boldsymbol{\delta}$ also influences convergence to the terminal states and are set as $\boldsymbol{k} = diag([1 \quad 1 \quad 1])$ and $\boldsymbol{\delta} = 0.01$. The adaptive parameters that influence the controller's performance and the convergence rate of the estimation of the unknown bounds c_1 and c_2 are defined as $\bar{\kappa}_1 = 0.0001$, $\bar{\kappa}_2 = 6 \times 10^{-7}$, $\bar{\kappa}_3 = 0.1$ and $\tau = 0.1$.

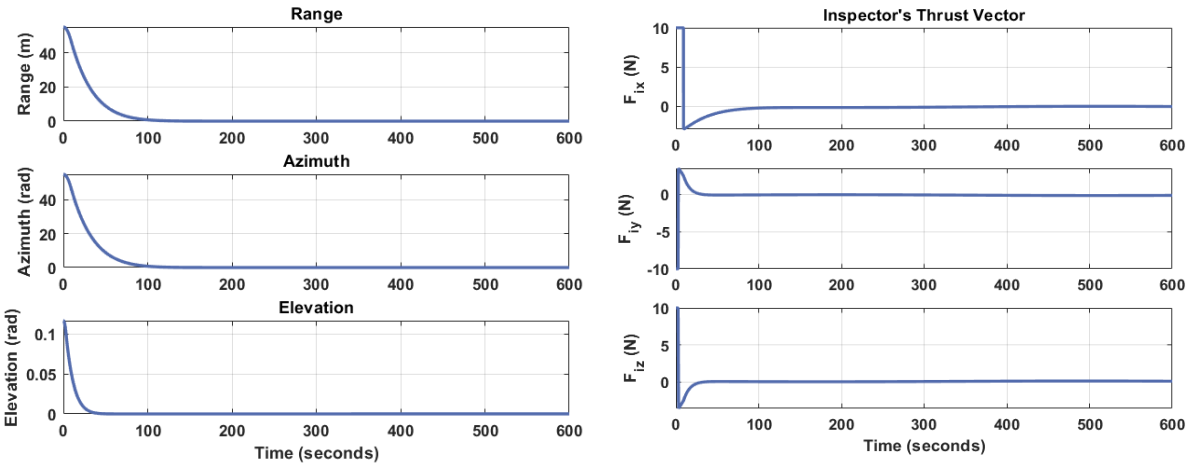

Figure 4: Inspector's error state (left) Inspector's thrust profile (right)

The rendezvous simulation is propagated for 600 s; the error state trajectories and the inspector's thrust profile are shown in **Figure 4**. The proposed ANTSMC law quickly converges to the desired states, despite the malfunctioning nature of the client, external disturbances and the inspector's thrust saturation. Initially the inspector's thrust profile is saturated as the controller works to reduce the systems tracking

Distribution Statement A. Approved for public release, distribution is unlimited.

error and force the system trajectories on to the sliding manifold; this effect only occurs during the first few seconds of the simulation at which point the control signal is attenuated.

The successful implementation of adaptation laws was also demonstrated, significantly improving the proposed controller's performance, and significantly reduce the control gain, which in turn drastically reduced the controller demand. During the simulation the adaptive gain will increase until the sliding mode is achieved, at which point the bounded uncertainties are deemed effectively counteracted and the adaptive gain is attenuated; this ability directly influences the performance of the controller, both in terms of control signal amplitude and convergence to the terminal states. Analyzing the control profile in **Figure 4**, it is clear that the adverse chattering phenomenon has been eliminated effectively with the proposed approach demonstrating that the ANTSMC algorithm can benefit from both high precision and chattering elimination.

Scenario 2:

To further demonstrate the effectiveness of the proposed ANTSMC law a rendezvous maneuver is simulated requiring the inspector to fly around a malfunctioning client; the desired terminal states are shown in **(13)**.

$$\boldsymbol{q_d} = \begin{bmatrix} 5\,m \\ 0.008\boldsymbol{t}\,rad \\ 0\,rad \end{bmatrix} \tag{13}$$

The sliding surface parameters are defined as $\alpha = diag([70 \quad 20 \quad 15])$ and $\lambda = 1.1$; the control parameter $\boldsymbol{k}$ and $\boldsymbol{\delta}$ are defined as $\boldsymbol{k} = diag([1 \quad 1 \quad 1])$ and $\boldsymbol{\delta} = 0.01$. The adaptive parameters are defined as $\bar{\kappa}_1 = 0.0003$, $\bar{\kappa}_2 = 1 \times 10^{-7}$, $\bar{\kappa}_3 = 0.1$ and $\tau = 0.1$.

The rendezvous simulation is propagated for 1200 s, long enough to achieve a full orbit about the client; the error state trajectories and the inspector's thrust profile are shown in **Figure 5** and the inspector's simulated rendezvous trajectory is shown in **Figure 6**. Despite the malfunctioning nature of the client, external disturbances and the inspector's thrust saturation, the proposed ANTSMC law quickly converges to the desired states, placing the inspector into a parking orbit about the client vehicle.

Similar to the first scenario the adaptation laws significantly improving the proposed controller's performance by attenuating the adaptive control gain throughout the simulation leading to significantly reduce controller demand that would otherwise negatively impact the inspector's ability to maintain a relative orbit about the client. As shown in **Figure 5**, the proposed control approach can effectively eliminate chattering effects during the simulation as well as maintain high precision despite tracking a moving trajectory.

Distribution Statement A. Approved for public release, distribution is unlimited.

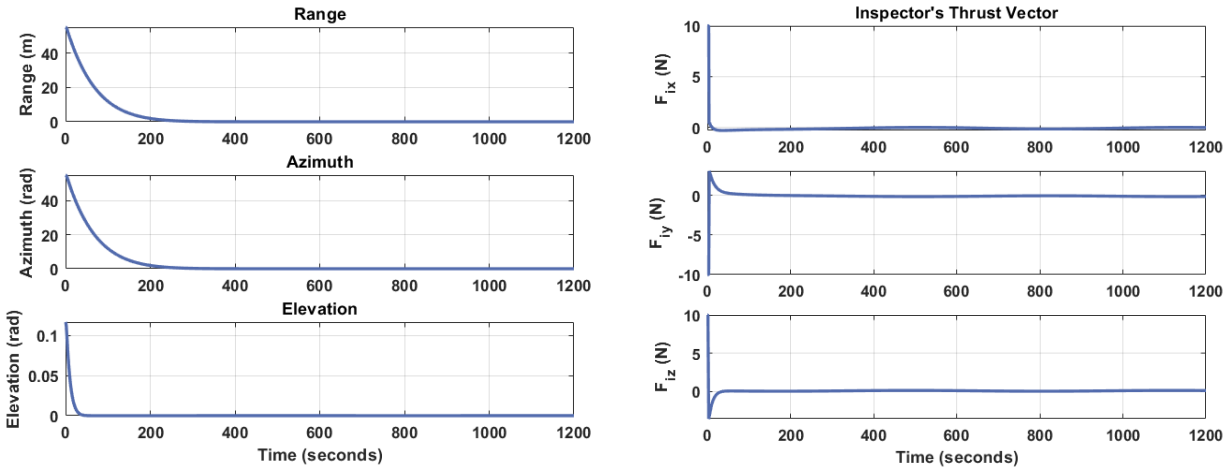

Figure 5: Inspector's error state (left) Inspector's thrust profile (right)

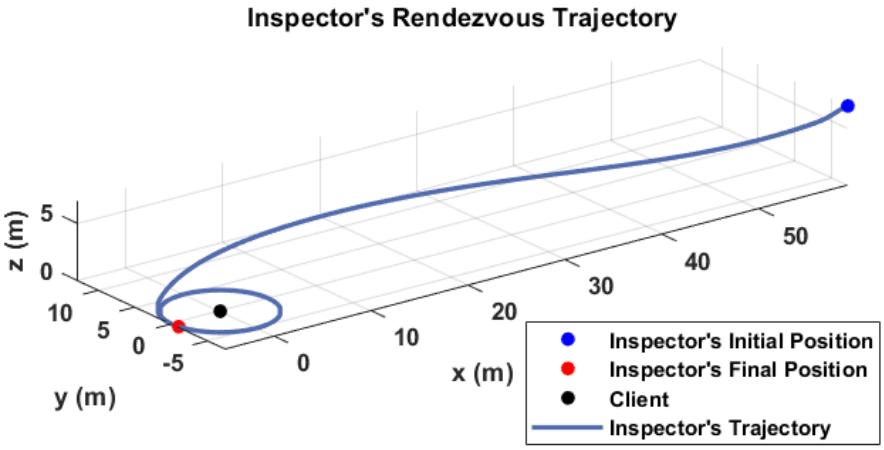

Figure 6: Inspector's Rendezvous Trajectory

Scenario 3:

The final scenario will demonstrate a far-range rendezvous maneuver using the proposed ANTSMC strategy; the client and inspector's orbital elements are shown in **Table 2**, derived using the user defined initial states, shown in **(14)**. The inspection vehicle is assumed to be larger (~300 kg) with higher thrust saturation of ± 300 N, the client is assumed smaller (~100 kg).

$$\boldsymbol{q_0} = \begin{bmatrix} 600\,m \\ -2.9848\,rad \\ 0.0017 rad \end{bmatrix}, \quad \dot{\boldsymbol{q}}_{\boldsymbol{0}} = \begin{bmatrix} 0.2695\,{}^{m}/_{s} \\ 1.0833 \times\ 10^{-3}\,{}^{rad}/_{s} \\ -0.2189 \times\ 10^{-4}\,{}^{rad}/_{s} \end{bmatrix} \tag{14}$$

Distribution Statement A. Approved for public release, distribution is unlimited.

	a (km)	e	i (°)	Ω (°)	ω (°)	Θ (°)
Client	7200	0.15	15	45	10	30
Inspector	7200.2	0.15	14.9999	45.0001	10	29.9945

Table 2: Client and inspector's orbital elements

To demonstrate the effectiveness of the proposed ANTSMC law for a far-range rendezvous maneuver the desired terminal states are first selected as shown in **(15)**.

$$\boldsymbol{q_d} = \begin{bmatrix} 20\ m \\ 0\ rad \\ 0\ rad \end{bmatrix} \tag{15}$$

The sliding surface parameters are set as $\alpha = diag([100 \quad 100 \quad 100])$ and $\lambda = 1.1$; the control parameter $\boldsymbol{k}$ and $\boldsymbol{\delta}$ are set as $\boldsymbol{k} = diag([1 \quad 1 \quad 1])$ and $\boldsymbol{\delta} = 0.01$ and the adaptive parameters are defined as $\bar{\kappa}_1 = 1.3 \times 10^{-4}$, $\bar{\kappa}_2 = 1 \times 10^{-9}$, $\bar{\kappa}_3 = 0.12$ and $\tau = 0.5$. These parameters can be tuned to achieve desirable performance. The error state trajectories and the inspector's thrust profile are shown in **Figure 7** with the inspector's rendezvous trajectory shown in **Figure 8**. This research has previously identified other sliding mode control designs that can accomplish this rendezvous procedure with similar results and are computationally less expensive; however, many of the identified manifolds do not contain the advantageous finite-time or nonsingular properties.

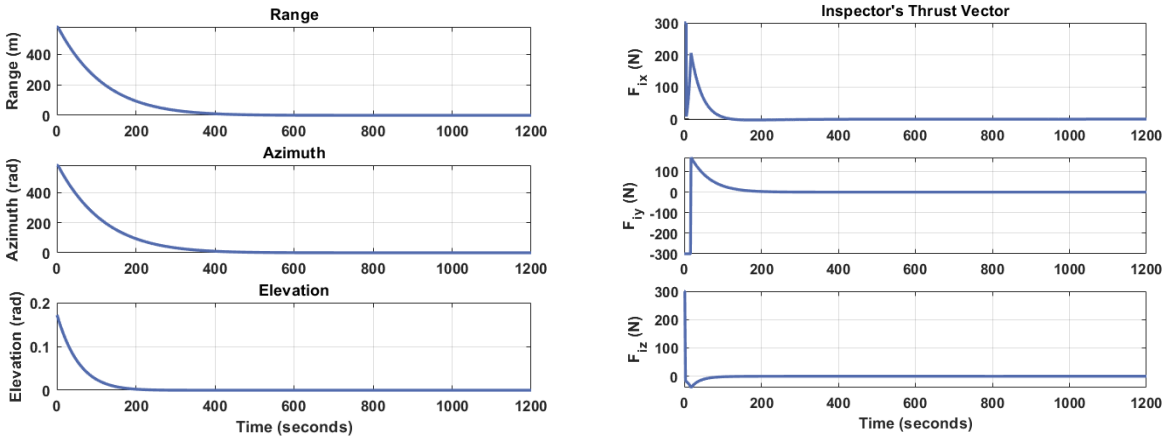

Figure 7: Inspector's error state (left) Inspector's thrust profile (right)

Distribution Statement A. Approved for public release, distribution is unlimited.

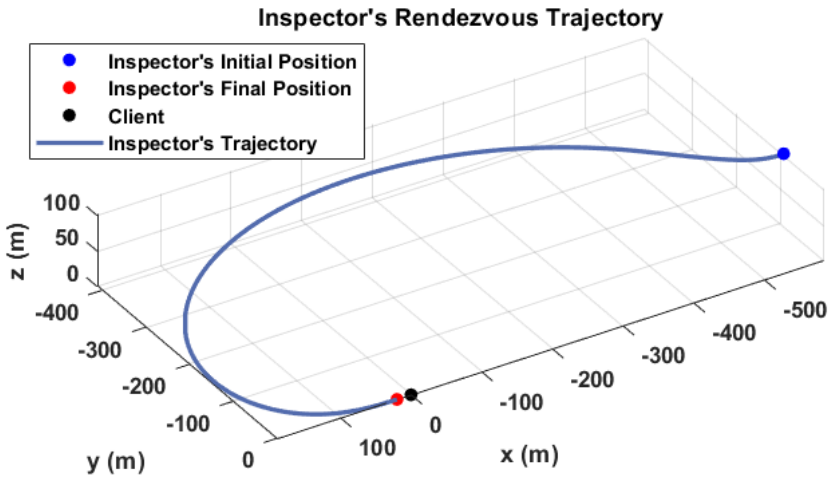

Figure 8: Inspector's Rendezvous Trajectory

CONCLUSIONS AND FUTURE WORK

On-orbit inspection of malfunctioning clients is a complex and challenging process, hampered by uncertainty and unpredictability; relevant technologies are still relatively new and underdeveloped and developing the capabilities that enable on-orbit inspection of malfunctioning clients is paramount to the future of space flight. Approaching a malfunctioning client is hazardous as the client is hindered from communicating real-time information, meaning the inspector relies solely on its on-board sensors suite to understand the behavior of the client. This is challenging considering the client could be uncontrollable, maneuvering unknown to the inspection vehicle *a-priori*. Unknown maneuvers could include both translational maneuvering and tumbling, introducing unique challenges that must be solved.

With the understanding that few attempts have been made in literature that address on-orbit inspection of malfunctioning clients this research investigated how to solve such a complex and challenging problem. The objective of this study was to develop a control simulation that demonstrated an inspection vehicle's capability to autonomously maneuver into a close proximity parking orbit about a malfunctioning client, hoping to fill an identified gap in literature and assist future research and development. This research focused on building simulation software to demonstrate the autonomous rendezvous and proximity maneuvering capabilities of an inspection vehicle when considering malfunctioning clients. Several scenarios were investigated including close range and far range rendezvous with varying terminal conditions.

This analysis has demonstrated that a LOS-based relative motion model can be used with an ANTSMC algorithm to maneuver an inspection vehicle into proximity of a client. This analysis first applied the suggested approach to close range rendezvous scenario with a malfunctioning client, hindered from communicating with an inspection vehicle, and demonstrated that the suggested approach achieves high

Distribution Statement A. Approved for public release, distribution is unlimited.

precession and finite time convergence despite the malfunctioning nature of the client vehicle; with chattering eliminated, improved control accuracy was also achieved. Similar observations are made when considering a far range rendezvous. The scenarios presented demonstrate the application of sliding mode control theory to uncertain nonlinear systems as well as the advantages of using a LOS-based relative motion model. The utility of using adaptive control theory to deal with bounded uncertainties was also demonstrated.

During the first year of this fellowship the necessary simulation software was developed to demonstrate autonomous rendezvous with malfunctioning clients to achieve a variety of desired final conditions. This simulation will be further developed over the next term of this fellowship. The capability to maneuverer an inspection vehicle within proximity of maneuvering clients has proven challenging and is still being developed; developing this capability and implementing it into the working simulation will be the focus of next year's research. It is also of interest to investigate client tumbling; currently, only a preliminary investigation into the effects of client tumbling has been completed. Future work will also include optimizing the simulation software for far range rendezvous scenarios, improving adaptation logic and investigating different manifold designs that contain the advantageous non-singular and finite-time properties. Finally, the intent of this research is to reach a conclusion on the feasibility of implementing the suggested approach on a real sortie, investigating the effects of malfunctioning or non-ideal thrusters could prove valuable; properly modeling external disturbances could also be of interest.

Distribution Statement A. Approved for public release, distribution is unlimited.